Journal of Hydrology 444–445 (2012) 134–145

Contents lists available at SciVerse ScienceDirect

Journal of Hydrology

journal homepage: www.elsevier.com/locate/jhydrol

Analysis and dynamic modeling of a moraine failure and glacier lake outburst flood at Ventisquero Negro, Patagonian Andes (Argentina)

Raphael Worni [a,b,*], Markus Stoffel [a,b], Christian Huggel [a,c], Christian Volz [d], Alejandro Casteller [b,e], Brian Luckman [f]

[a] Institute for Environmental Sciences, University of Geneva, route de Drize 7, CH-1227 Carouge, Switzerland
[b] Institute of Geological Sciences, University of Bern, Baltzerstrasse 1-3, CH-3012 Bern, Switzerland
[c] Department of Geography, University of Zurich–Irchel, Winterthurerstrasse 190, CH-8057 Zurich, Switzerland
[d] Laboratory of Hydraulics, Hydrology and Glaciology (VAW), ETH Zurich, Gloriastrasse 37-39, CH-8006 Zurich, Switzerland
[e] Instituto Argentino de Nivología, Glaciología y Ciencias Ambientales (IANIGLA), CONICET, C.C. 330, 5500 Mendoza, Argentina
[f] Department of Geography, University of Western Ontario, 1151 Richmond Street, London, Ontario, Canada N6A 5C2

ARTICLE INFO

Article history:
Received 16 August 2011
Received in revised form 3 January 2012
Accepted 8 April 2012
Available online 17 April 2012
This manuscript was handled by Konstantine P. Georgakakos, Editor-in-Chief, with the assistance of Ehab A. Meselhe, Associate Editor

Keywords:
Moraine breach
Glacier lake outburst flood (GLOF)
Ventisquero Negro (Patagonia)
Dam break modeling
BASEMENT
Outburst hydrograph

SUMMARY

Although moraine dams are inherently prone to failure because of their often weak structure, loose internal composition and lack of an engineered spillway, the understanding of dam breaching processes remains largely incomplete and appropriate modeling approaches are scarce. This paper analyzes a recent glacier lake outburst, caused by the failure of the terminal moraine of Ventisquero Negro (Patagonian Andes, Argentina) in May 2009. The dam breach trigger, breaching and lake emptying processes, plus the dynamics of the outburst flood were reconstructed based on field evidence and the application of a dynamic dam break model. Results indicate that the moraine failure was caused most probably by a rising lake level due to heavy precipitation, resulting in high lake outflow which led to dam erosion and finally to dam failure. The lake volume of ca. 10×10^6 m^3 was released in ca. 3 h, producing high-discharge (ca. 4100 m^3 s^{-1}) debris flows and hyperconcentrated flows as the escaping water entrained large volumes of clastic material. The methodology presented in this paper provides valuable insights into complex dam breach and GLOF processes, and closes a critical gap in dynamic dam break modeling aimed at providing the lake outburst hydrograph. An accurate determination of outburst hydrographs constitutes one of the most crucial aspects for hazard assessment of unstable lakes and will gain further importance with ongoing glacier retreat and glacier lake formation.

© 2012 Elsevier B.V. All rights reserved.

1. Introduction

Glaciated high-mountain regions are particularly susceptible to climate change (IPCC, 2007) and associated changes in hazard situations (Stoffel and Huggel, 2012). Recent glacier melt has given rise to the formation of moraine-dammed glacier lakes (Clague and Evans, 2000), which typically form between the glacier snout and end moraines during periods of glacier retreat (Costa and Schuster, 1988). Moraine dams are inherently prone to failure because of their often weak structure, loose internal composition and lack of an engineered spillway. Sporadic glacier lake outbursts may drain as powerful floods (Mergili et al., 2011) and are considered the most important glacier-related hazard in terms of direct damage potential (Osti and Egashira, 2009). Glacier lake outburst floods (GLOFs) have killed thousands of people in many parts of the world (Clarke, 1982; Hewitt, 1982; Clague and Evans, 1994, 2000; Watanabe and Rothacher, 1996; Richardson and Reynolds, 2000a; Huggel et al., 2004; Carey, 2005) and with ongoing glacier retreat new, often unstable glacier lakes are likely to develop in the future (Frey et al., 2010). As a result GLOF risks are receiving increased attention as a key climate change hazard (Malone, 2010).

The stability of a moraine dam has been shown to depend primarily on its geometry, internal structure, material properties and particle-size distribution (Costa and Schuster, 1988; Richardson and Reynolds, 2000b; Korup and Tweed, 2007). Melting of stagnant ice within ice-cored moraine dams has been reported to create conduits for lake water to percolate into moraines, contributing to a weakening of overall dam structure (Clague and Evans, 2000; Richardson and Reynolds, 2000b). However, most moraine-dammed

* Corresponding author at: Institute of Geological Sciences, University of Bern, Baltzerstrasse 1-3, CH-3012 Bern, Switzerland. Tel.: +41 (0)31 631 52 79; fax: +41 (0)31 631 48 43.
E-mail addresses: raphael.worni@dendrolab.ch (R. Worni), markus.stoffel@dendrolab.ch (M. Stoffel), christian.huggel@geo.uzh.ch (C. Huggel), volz@vaw.baug.ethz.ch (C. Volz), casteller@mendoza-conicet.gob.ar (A. Casteller), luckman@uwo.ca (B. Luckman).

0022-1694/$ - see front matter © 2012 Elsevier B.V. All rights reserved.
http://dx.doi.org/10.1016/j.jhydrol.2012.04.013

lakes do not burst catastrophically. At the same time, dams that are considered stable do not necessarily prevent disasters either, as was the case at Laguna 513, a glacier lake in the Cordillera Blanca of Peru, where a displacement wave (induced by an ice avalanche) caused water to overtop a bedrock dam and caused an outburst flood in 2010 (Carey et al., 2011). Moraine dams fail when the material strength of the dam is exceeded by driving forces that comprise, among others, the weight of the impounded water mass, seepage forces and shear stresses from overtopping flow or displacement waves (Korup and Tweed, 2007; Massey et al., 2010). Overtopping flows can be caused by heavy rainfall or a sudden influx of water from upstream sources; displacement waves are, in contrast, triggered by mass movements e.g. snow and ice avalanches, rockfalls, debris flows or landslides, entering the lake (Costa and Schuster, 1988; Clague and Evans, 2000; Huggel et al., 2004). Once the lake overflows water will typically induce dam erosion, forming an initial breach, that leads to greater outflow and increasing hydrodynamic forces that cause progressive breach enlargement (Singh, 1996). Critical shear forces on the dam material are exerted by the flow and the eroded sediments are transported downstream as bedload. This process is irreversible and will ultimately lead to a partial or complete emptying of the glacier lake.

Before structural, land-use planning or emergency-oriented prevention measures can be undertaken to reduce the risks from GLOFs, the dimensions of an expected outburst flood must be evaluated. Hydraulic flood models are valuable tools for quantitative assessment of large-scale floods and a key instrument for the assessment of GLOF hazards and the planning of prevention measures (Valiani et al., 2002; Jorgenson et al., 2004; Worni et al., 2011).

One of the most crucial model input parameter for such assessments is the flood hydrograph, which reflects discharge per unit time. The hydrograph of a lake outburst flood can be approximated with empirical relationships (Evans, 1986; Huggel et al., 2004; Kershaw et al., 2005) or calculated using empirical and physical dam break models. Empirical dam break models use analytically-solved equations derived from past dam breach events with known breach dimensions and expansion rates (Singh, 1996). Physical models apply geotechnical considerations, erosion rates and hydraulic principles to take account of breach development. However, many physical dam break models (e.g. BREACH, Fread (1991) or BEED, Singh and Scarlatos (1985)) still require critical input parameters regarding the shape of the breach and its enlargement over time, which are often based on assumptions rather than on physical evidence, rendering these programs less site-specific (Hahn et al., 2000; Volz et al., 2010; Pickert et al., 2011). Recently, new erosion-based dynamic models (Faeh, 2007; Balmforth et al., 2008; Faeh et al., 2011) have been developed, which represent a promising approach to capture breaching processes with good accuracy. These models solve balancing equations for water and sediment flow in combination with empirical transport formulas to simulate embankment failures, thereby using clear physical input parameters.

No matter which approach is applied to calculate future outburst scenarios of unstable glacier lakes or other dam breaches, model calibration and validation based on past events remain crucial (Clarke, 1982; Meon and Schwarz, 1993; Walder and Costa, 1996; Tingsanchali and Chinnarasri, 2001). This is challenging as little is known about outburst mechanics and the hydrodynamic characteristics of GLOFs, because many past moraine breaches and subsequent lake outburst floods often went unrecorded and in remote areas (Carrivick et al., 2009; Osti and Egashira, 2009). Therefore the moraine failure and lake drainage event at Ventisquero Negro (Mount Tronador, Patagonian Andes, Argentina) is an important contribution to the analysis of dam failures and GLOF processes, and an ideal case to calibrate and test dam break models.

The purpose of this study is to (i) reconstruct the moraine breaching, lake emptying and flood propagation processes of the Ventisquero Negro GLOF based on field evidence; and to (ii) apply and test the dynamic, erosion-based dam break model BASEMENT (Faeh et al., 2011). This reveals valuable quantitative insights into dam breaching and lake emptying processes that are rarely available from other GLOF events, and closes a critical gap in dynamic moraine breach modeling for which few detailed studies exist (e.g. Hancox et al., 2005; Balmforth et al., 2008; Xin et al., 2008).

2. Study area

Mount Tronador (41°10′S, 71°52′W; 3480 m asl) is the highest mountain in Nahuel Huapi National Park and straddles the border between Chile and Argentina in northern Patagonia. The upper part of the mountain is covered by a continuous ice cap, with eleven outlet glaciers. The total glacier area is about 64 km^2 and the largest glaciers reach down to 950 m asl, well below the local tree line of ~1700 m asl (Villalba et al., 1997).

The Rio Manso valley glacier in Argentina flows down the south-eastern flanks of Mount Tronador and is separated by a steep cliff several hundred meters high from the main ice cap. The glacier is fed by snow, ice and debris avalanches from the steep slopes above. Due to a thick debris layer covering large portions of its ice, the Rio Manso valley glacier is locally known as Ventisquero Negro, meaning black glacier. Ventisquero Negro is constrained by a massive terminal moraine with a fork-like shape, forming the Rio Manso outlet at its lowermost point (Fig. 1). During the Little Ice Age, the glacier partly overtopped the older (>2000 year old) end moraine and subsequent glacier recession resulted in a debris-covered ice body abutting the inner slope of the end moraine (Masiokas et al., 2010).

Documentary evidence, satellite imagery and aerial photographs indicate that the glacier margin varied relatively little between 1937 and 1991. However, rapid thinning and recession of the glacier tongue was observed between the early 1990s and the present (Masiokas et al., 2010). The 1981 aerial photograph and a SPOT5 image from December 2008 (Fig. 1) illustrate the mass and length losses at Ventisquero Negro. The recession of Ventisquero Negro resulted in the formation of a proglacial lake between the end moraine and the glacier fronts. The lake grew rapidly after the 1990s and the SPOT5 image from 2008 shows the maximum lake extent with an area of ca. 47 ha before the moraine breach in May 2009. The damaged moraine and emptied lake can be seen on the GeoEye satellite image taken in November 2010 (Fig. 1). On its way to Mascardi Lake, located 22 km downstream of the glacier lake, the Rio Manso crosses the small settlement and tourist resort of Pampa Linda (ca. 7 km below the glacier lake).

3. Geomorphic, ground observation, and meteorological data

In February 2010, field work was carried out to analyze the residual Ventisquero Negro glacier lake, the breached moraine and the flooded Manso valley. The goal was to gather data on the dam, breach, and (former) lake geometry, the structure and material composition of the end moraine, and wetted cross-sections in the Manso valley.

The mapping of the lake, moraine and breach was carried out using a Tech-Geo GTR differential GPS and a Nikon LASER 550A S high-specification laser distance measurement tool with an integrated angle measurement function. Ground measurements were

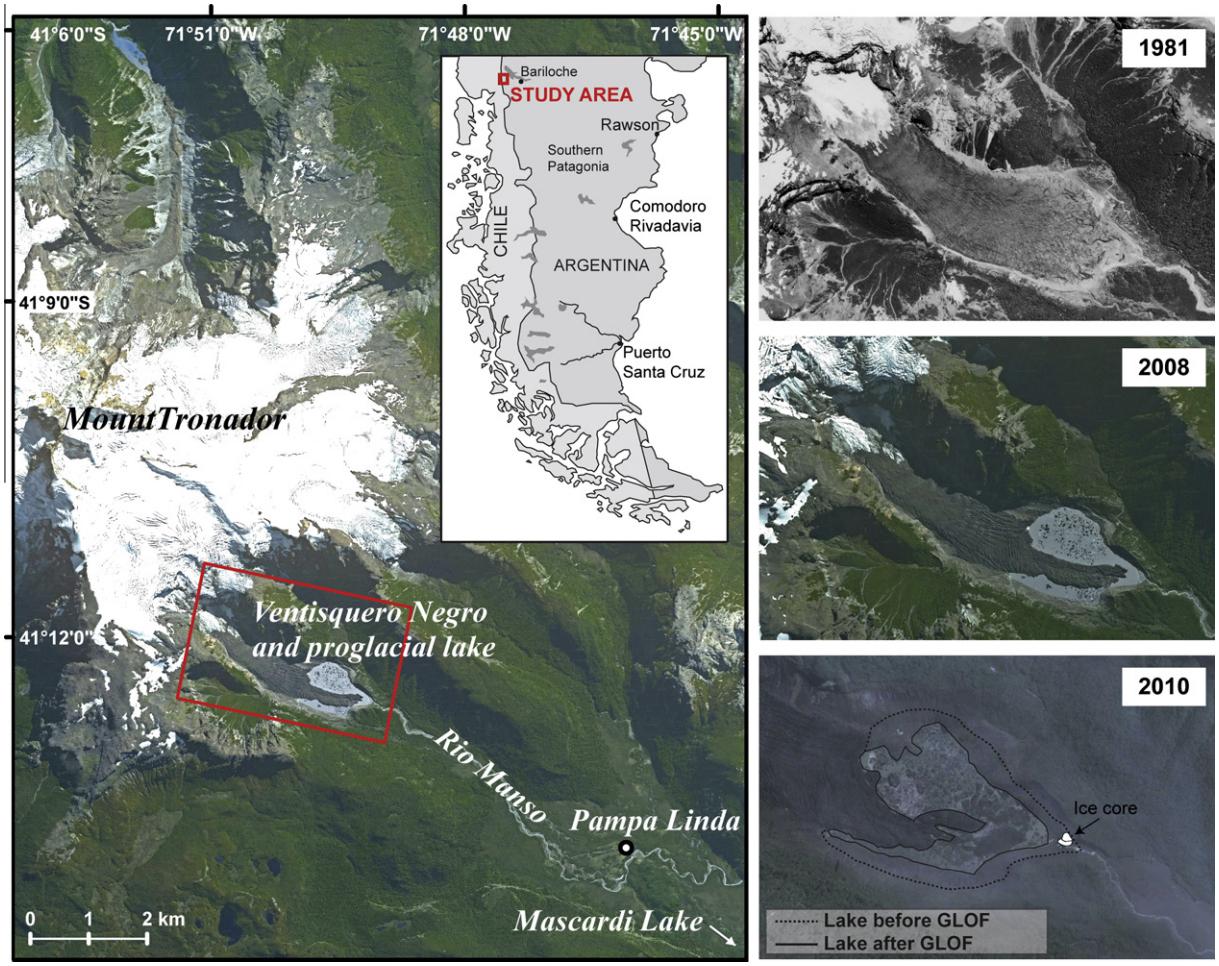

Fig. 1. Mount Tronador and Ventisquero Negro, its proglacial lake and the Rio Manso valley in Northern Patagonia, Argentina. A SPOT5 satellite image from December 2008, a GeoEye satellite image from November 2010 (extracted from GoogleEarth) and an aerial photograph from 1981 (IANIGLA) illustrate the recession and thinning of Ventisquero Negro and the formation and failure of its proglacial lake.

complemented by data from satellite imagery and aerial photographs. A pre-GLOF SPOT5 satellite image of 2.5 m resolution and a post-GLOF GeoEye satellite Image with a 1.65-m resolution were extracted from GoogleEarth and georeferenced. Additionally, LANDSAT ETM+ imagery from April 2009 and an ALOS scene from March 2010 were used to document and map breach geometry and geomorphic changes before and after the GLOF. Aerial photographs from 1970 and 1981 were used to reconstruct recent glacier dynamics at Ventisquero Negro and lake formation, and to generate a digital elevation model (DEM) with a 7-m resolution of Ventisquero Negro and the Rio Manso area. Absolute and relative vertical accuracies of the DEM are ±24 m and ±4 m, respectively, based on a comparison of elevations using the DEM and GPS measurements.

Six hour-interval precipitation data from May 2009 and monthly precipitation data from 1985 to 1997, measured at the rain gauge at Lake Mascardi (22 km downstream of Ventisquero Negro), were analyzed to document the role of rainfall in the triggering of the dam breach. In addition, monthly precipitation data from 1905 to 2006 were available for Bariloche (45 km from Ventisquero Negro), as well as daily precipitation data from 1971 to 2005 from Lake Gutierrez (35 km from Ventisquero Negro). A strong W to E precipitation gradient exists between Ventisquero Negro and Bariloche/Lake Gutierrez (Villalba et al., 1997), but these longer records are useful to put the shorter, proximal records into a regional climatic context and extend the rainfall record into 21st century.

4. Modeling approach

4.1. Dam break model

The two-dimensional numerical model BASEMENT (Faeh et al., 2011) was used to investigate the breaching process of the Ventisquero Negro end moraine and the related lake drainage. The program is initially based on the existing 2dMB model, which has been applied successfully to breaching processes of earth embankments (Faeh, 2007). BASEMENT has been designed as a tool for the analysis of breaching processes of non-cohesive earthen dam structures and water-sediment flows (Volz et al., 2010). The 2D shallow water equations (1) and (2) are general constitutive flow equations, and are solved with an explicit Finite-Volume method on unstructured meshes. The primary variables are water depth h and specific discharges ($q = uh$, $r = vh$) in the coordinate directions.

$$\frac{\partial h}{\partial t} + \frac{\partial (uh)}{\partial x} + \frac{\partial (vh)}{\partial y} = 0 \tag{1}$$

$$\begin{aligned} \frac{\partial}{\partial t}(hu) + \frac{\partial}{\partial x}\left(hu^2 + \frac{1}{2}gh^2\right) + \frac{\partial}{\partial y}(huv) &= -gh\frac{\partial z_B}{\partial x} - \frac{\tau_{Bx}}{\rho} \\ \frac{\partial}{\partial t}(hv) + \frac{\partial}{\partial x}(huv) + \frac{\partial}{\partial y}\left(hv^2 + \frac{1}{2}gh^2\right) &= -gh\frac{\partial z_B}{\partial y} - \frac{\tau_{By}}{\rho} \end{aligned} \tag{2}$$

where u is the velocity in x direction, v is velocity in y direction, g is the gravitational acceleration, ρ is the fluid density, z_B is the bottom elevation. The bed shear stresses (τ_{Bx}, τ_{By}) act in the direction of

depth-averaged velocities and are determined using the quadratic resistance law with c_f being the dimensionless friction factor as

$$\tau_{Bx} = \rho\sqrt{u^2+v^2}u/c_f^2, \quad \tau_{By} = \rho\sqrt{u^2+v^2}v/c_f^2 \tag{3}$$

The hydraulic fluxes are calculated using an exact Riemann solver (Toro, 2001), which leads to an accurate and stable simulation scheme even for very unsteady flow conditions and changing flow regimes, which have to be expected during dam breaching. The model's capacity to handle moving boundaries and drying–wetting fronts appropriately is of special importance for dam break simulations.

Erosion and transport of dam material due to overtopping flow is calculated with empirical sediment transport equations. The program evaluates surface erosion based on the bottom shear stress exerted by the flow on the dam material. Thus, sediment transport laws are used to determine vertical incision in earthen dam structures. Thereby a layer-approach is applied, i.e. grain sorting takes place in the uppermost (mixing) layer and additional sediment layers can be defined over depth with different compositions. In case of fractional transport the sorting equation (4) needs to be solved for each grain class g,

$$(1-p)\frac{\partial}{\partial t}(\beta_g \cdot h_m) + \frac{\partial q_{Bg,x}}{\partial x} + \frac{\partial q_{Bg,y}}{\partial y} - s_{fg} = 0 \tag{4}$$

and the total sediment mass balance (5) is obtained by summing all sediment fluxes,

$$(1-p)\frac{\partial z_B}{\partial t} + \sum_{g=1}^{ng}\left(\frac{\partial q_{Bg,x}}{\partial x} + \frac{\partial q_{Bg,y}}{\partial y}\right) = 0 \tag{5}$$

where β_g is the fraction of grain class g, h_m is the thickness of the control volume,[1] p is the porosity of sediment, and where $q_{Bg,x}$ and $q_{Bg,y}$ are components of transport rate. The bed level z_B and the grain fractions β_g are the primary variables of sediment transport. The source term s_{fg} describes the exchange of sediment particles between the control volume and the underlying soil layer (Faeh et al., 2011). For erosion, material from the underlying soil layer of composition β^{sub} enters the control volume. For deposition, material leaves the control volume and enters the soil layer. With z_F as the bottom elevation of the control volume and z_{sub} as the bottom elevation of the underlying layer, the source term s_{fg} becomes

$$s_{fg} = -(1-p)\frac{\partial}{\partial t}[(z_F - z_{sub})\beta] \text{ with } \begin{cases} \beta = \beta_g & \text{for depostion} \\ \beta = \beta_g^{sub} & \text{for erosion} \end{cases} \tag{6}$$

Within this study, the transport rate was determined using a modified Meyer-Peter and Müller (Meyer-Peter and Müller, 1948) formula (7) for fractional transport with the hiding function[2] ξ after Ashida and Michiue (1971) and the critical bottom shear stress of incipient motion τ_{Bcr} from the shields-diagram (Shields, 1936).

$$q_{Bg} = \beta_g\left(\frac{\tau_B - \xi_g\tau_{Bcr,g}}{0.25\rho}\right)^{3/2}\left(\frac{1}{(\rho_s/\rho - 1)g}\right) \tag{7}$$

The complex geotechnical processes of lateral breach widening due to slope collapses of the side walls are considered with a geometrical 3D bank failure operator, which is based on three different critical failure angles: (i) a failure angle for dry or partially saturated material at the breach side walls above the water surface which can exceed the angle of repose due to the stabilizing effects of negative pore pressures; (ii) a failure angle for bank material below the water surface, which is fully saturated. This failure angle is expected to be in the range of the angle of repose; (iii) a failure angle for deposited material resulting from slope collapses. It approximates the sliding of the collapsed material into the breach channel after failure and determines the soil's redistribution in the breach channel. The deposition angle is not a pure material property, and therefore needs calibration.

If one of the failure angles is exceeded due to vertical erosion, gravitational bank failure is expected to occur and the slope is flattened until the critical angles are reached. The material moves in downward direction of the cell's slope and is added to transport rates.

4.2. Computational domain

The model domain for the dam break simulation (i.e. lake, moraine, and flood plain) was discretized with a 2D unstructured mesh. To ensure mass conservation, BASEMENT uses a separate mesh for sediment calculations, which is constructed automatically from the given mesh. The Surface Water Modeling System (SMS) software (SMS, 2012) was used to create the computational mesh consisting of ca. 29,000 triangular cells. For a flexible adaptation to local geometry variable cell sizes and local mesh refinements were applied. Based on satellite imagery the mesh was drawn in planar view and then height information from the DEM was interpolated on the mesh nodes. Although the DEM represents the terrain in 1981, dam geometry has not changed significantly over the past 30 years, but glacier and glacier lake geometry had to be corrected significantly with field data and satellite imagery due to glacier retreat.

5. Field-based reconstruction of the moraine failure and lake outburst flood

The breach of the Ventisquero Negro end moraine on 21 May 2009 produced a lake outburst flood that devastated the Rio Manso Valley. According to eyewitness reports, the resulting sediment-laden turbulent flow hit Pampa Linda (7 km downstream of the lake) at around 10.30 pm and lasted 7 ± 2 h. Data from field reconnaissance show that the lake water level dropped by ca. 27 m during the moraine failure and that <5 m of water height remained in the basin. Together with the reconstructed lake bathymetry from satellite imagery before and after the GLOF and field survey, the volume of released water was calculated as ca. 10×10^6 m^3. The moraine breach revealed buried glacier ice lying against the inner flank of the terminal moraine on the orographic left side of the breach.

5.1. Properties of the moraine breach and outburst flood

The end moraine of Ventisquero Negro contains non-cohesive, unconsolidated and poorly sorted granular materials consisting largely of coarse, blocky and bouldery material with a matrix of sand and gravel. Grain size distribution of moraine material was performed for sediments of the sidewalls inside the breach and defined by classical dry-sieving (0.125–2 mm) for the finer and photogrammetric analysis (2–1000 mm) for the coarser fractions (Fig. 2). The slope angle of the moraine wetted by the lake before the GLOF was 40–45°, which corresponds to the natural repose angle of the moraine; this value also served as a guideline for the failure angle below the water surface. The walls inside the breach after the GLOF had slope angles of up to 80–90° and indicate a possible value for the failure angle above the water surface.

The 350-m long breach (Fig. 3A) has minimum and maximum cross-sectional areas of 1100 and 2500 m^2, respectively. The

[1] Also known as mixing layer, which is the uppermost layer where bed load transport occurs (Faeh et al., 2011).

[2] The hiding function considers effects of hiding and exposure of the grain particles with different sizes at fractional transport.

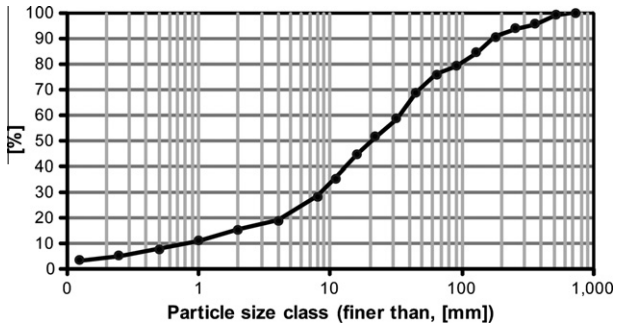

Fig. 2. Grain size distribution of moraine material as measured at the sidewalls inside the breach.

narrowest section of the breach is located at its upper end where an ice core (Fig. 3C) limits the width of passage to 12 m at the river bottom and to ca. 60 m at the top of the ice core, ca. 25 m above the present river bed. Downstream of the ice core the breach widens to an average cross-sectional width of 70 m, with a maximum of 120 m at the lowermost end of the moraine body. In the upper, central and lower segments the breach is about 50, 30 and 10–20 m deep, respectively (Fig. 3 overview). Breach volume (i.e. the amount of material eroded from the moraine dam) is ca. 230,000 m^3.

The flood deposits of the Ventisquero Negro GLOF provided information about flow behavior and flow type. Debris flow levees with overlying rocks of up to 6 m in diameter (*A* axis) indicate that the outflowing lake water entrained moraine material to form a debris flow in the uppermost reaches of Rio Manso (Fig. 3D). Deposition *en masse* and terminal lobes some 350 m downstream of the breach mark the point where this first debris flow surge stopped. Below this point, the GLOF flowed for 150 m as a sediment-laden flow, which was indicated by the absence of significant deposition or erosion traces and the presence of pre-flood vegetation. According to field deposits, at 500 m downstream of the breach, the surge evolved again into a debris flow, transporting and depositing material downstream on relatively flat terrain (ca. 2° decline). Maximum grain sizes and levee heights decreased with increasing flow distance and terminal lobes at ca. 1000 m below the breach clearly indicate the runout zone of the second debris flow surge (Fig. 3 overview). The total approximate volume of the debris flows was assessed at ca. 250,000 m^3, which corresponds to the amount of eroded moraine material. Below the deposition area of the second debris flow, flow traces indicate that the GLOF propagated downstream as a hyperconcentrated flow to become a stream flow before entering Mascardi Lake.

In the first 10 km the outburst flood changed flood plain morphology significantly by removing entire forest stands (Fig. 3E and F) and rocks. After 4 km, the flood diverged from the main river channel and flooded an area of approximately 1 km^2. Part of the water flowed along the road to Pampa Linda where a bridge and parts of the road were destroyed, while a camp ground and houses were partly flooded. Downstream of Pampa Linda the channel of Rio Manso was able to accommodate most of the released lake water.

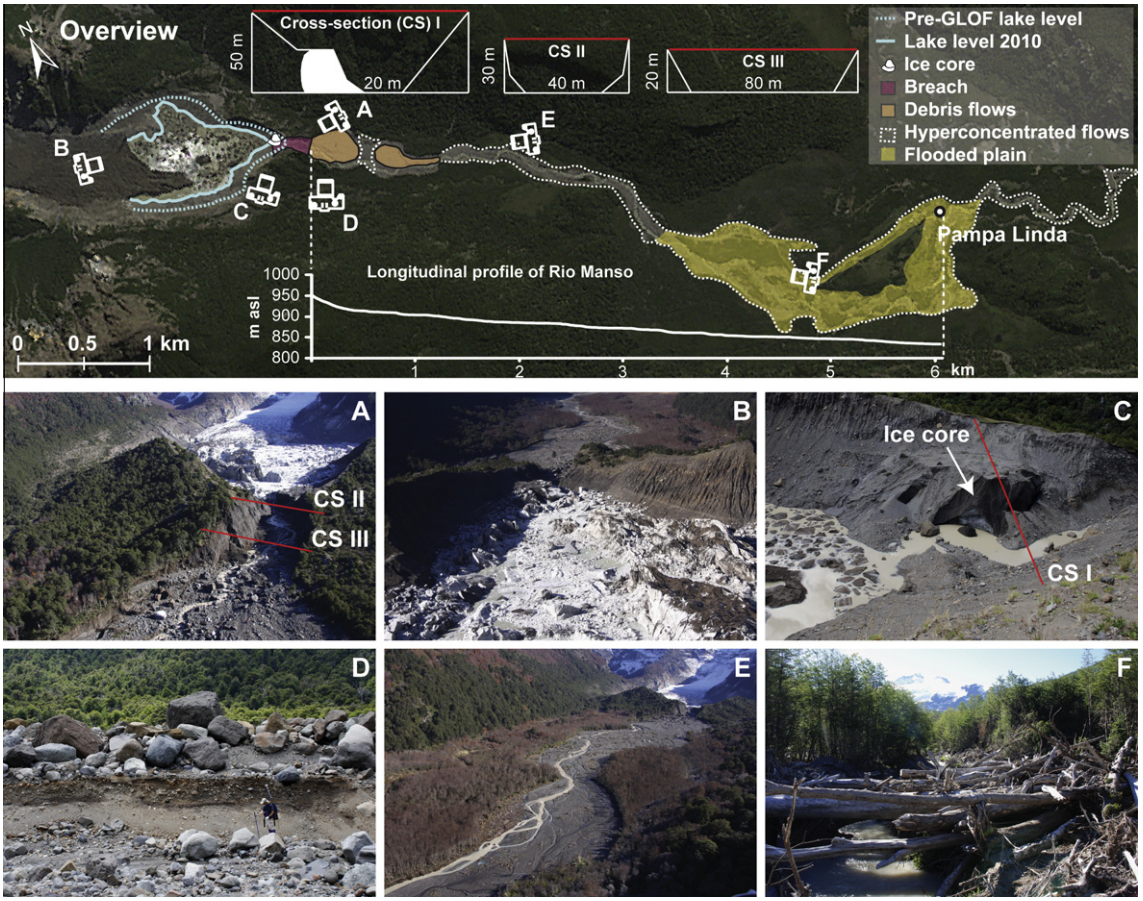

Fig. 3. In the overview, flow type of the GLOF, inundated area, the moraine breach, the ice core and actual and former lake outline are illustrated, and the positions of pictures (A–F) are indicated. In addition, a longitudinal profile of the study reach and three cross-sections of the breach are provided. Pictures (A), (B) and (E) were taken shortly after the GLOF from a helicopter and show (A) the moraine breach, (B) the emptied lake and (E) the flooded area, respectively (Club Andino Bariloche, used with permission). The other pictures were taken during the field campaign and illustrate (C) the buried ice core, (D) debris flow deposits close to the moraine and (F) trees transported along the flow path.

5.2. Dam breach trigger and dam failure processes

Meteorological records from Lake Mascardi report unusually heavy rainfall (total 170 mm) with high temperatures (mean daily temperature = 7 °C) during the six days prior to the outburst. Both the length and the intensity (50 mm in 48 h preceding the GLOF) of the rainfall event were among the highest reported for the station and also for Bariloche (Fig. 4). As the glacier lake is located 16 km away from the meteorological station, precipitation totals and patterns might have been different at Ventisquero Negro. However, park rangers reported that heavy rainfalls occurred at Ventisquero Negro as well; and that these rainfalls would have increased the level and outflow of the glacier lake. As a further consequence, ice blocks originating from glacier calving were uplifted and subsequently floated towards the outlet.

The increasing lake level and lake outflow most likely induced the moraine failure, as other possible trigger mechanisms could be excluded due to the absence of traces of mass-wasting events impacting the lake. The influence of an ice core >25 m in diameter against the inner slope of the moraine is of particular interest regarding both initiation of dam failure and breach formation. In principle, three different failure scenarios (or a combination of several of these scenarios) are possible:

Scenario 1: Intense rainfall resulted in increased lake overflow discharge. In this case, an unusual high lake outflow was sufficient to break the armor layer of the outlet river bed and to initiate vertical dam erosion. After initial incision, more lake water was able to flow out with a subsequent increase in sediment transport rates and a progressive expansion of the breach.

Scenario 2: High lake level and outwards current caused stranded ice blocks in the lake to uplift and drift toward the outlet. The ice plugged the outlet, ponding the lake to an even higher level. Due to the resulting increase in water pressure the ice blocks were abruptly washed away and the critical shear stress to initiate erosive processes was exceeded by the released water. Once the erosion started, breach expansion continued until the force of outflowing lake water decreased such that bedload was no longer transported.

Scenario 3: The rising water level of the lake resulted in increased hydrostatic pressure on the dam, which ultimately led to instability of the ice core abutting the moraine (by uplift caused by the hydrostatic gradient, by partially breaking apart, or by gradual melting as a result of water infiltration). The ice body acted as a barrier between the lake and the moraine and consequently, a destabilization of the ice core led to a destabilization of the moraine. The water pressure caused partial collapses of the moraine body leading to more sudden lake emptying than in scenarios 1 and 2 (Fig. 5).

6. Modeling the moraine failure and lake emptying

6.1. Model setup

Moraine breach modeling started with a semi-quantitative sensitivity analysis of several hydraulic and morphologic model parameters. The sensitivity of model parameters on simulation output was tested by varying their value within a reasonable range (Table 1) while maintaining all other parameters at default values. Then the change of modeled discharge and breach erosion before and after parameter variation was analyzed. Parameter sensitivity was considered small when the influence on modeled discharge and erosion was <10%, moderate if 10–25% and high if >25%.

Most of these parameters given in Table 1 were directly measured in the field, others are typical material constants. The bedload factor, control volume thickness and deposition failure angle were difficult to derive but were required for the simulation and serve to some extent as calibration factors.

Lake bathymetry (represented by the mesh created in SMS) and water surface elevation prior to the lake outburst defined BASEMENT's initial condition (Fig. 6). The sudden release of water from the lake and an associated high outflow right from the start of the model run were possible through the definition of a water surface elevation above the lake outlet. Such initial conditions might have existed at the study site due to an abrupt removal of ice blocks that temporarily dammed the lake (scenario 2). Once water is flowing, the hydrostatic force of the lake is the main driver for continuous outflow and dam erosion. In the present case, the initial water surface elevation had to be >2 m above the outlet to provoke sufficient initial bedload transport and to maintain breach expansion and lake emptying. An external water source of 25 $m^3 s^{-1}$ was defined as an additional upper boundary condition, representing water inflow from ice melt and precipitation. However, this estimated lake inflow hydrograph had minimal influence on the dam breach process.

The moraine dam was defined to consist of erodible sediments with material properties, material failure angles and grain size distribution as defined in Table 1. The ice core lying against the inner flank of the moraine was replaced by erodible dam sediment,

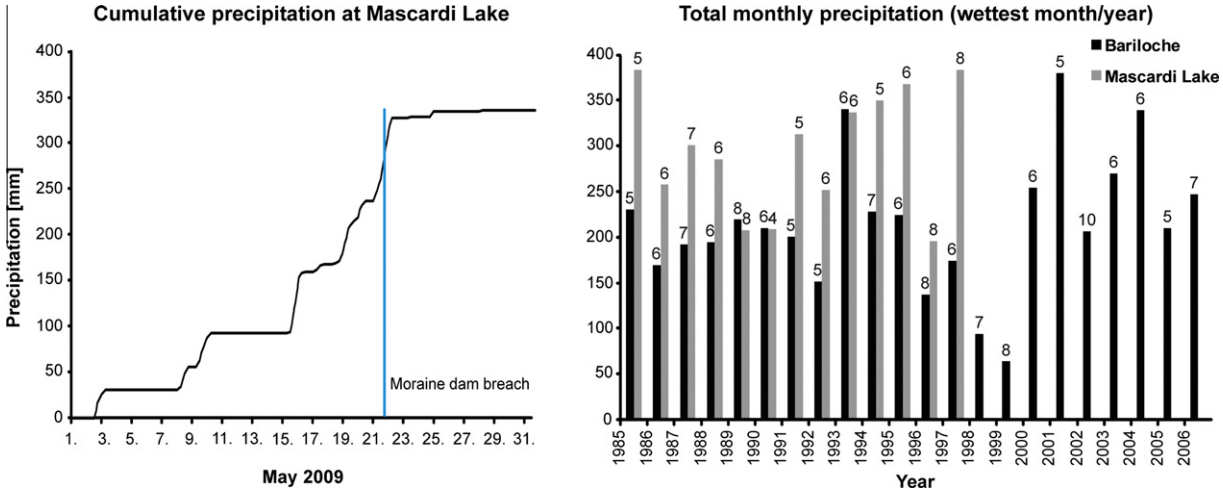

Fig. 4. Cumulative precipitation measured at 6 h intervals at the rain gauge station at Mascardi Lake during May 2009 (black curve). From the same station total monthly precipitation data are available from 1985 to 1997 (gray bars). Total monthly precipitation data from 1985 to 2006 from Bariloche are included in the graph (black bars). For each year the wettest month was plotted; numbers above the bars indicate months from April (4) to October (10).

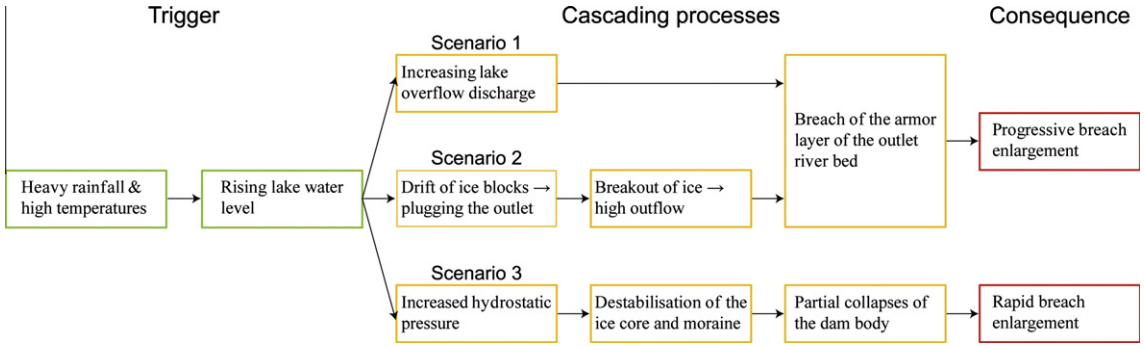

Fig. 5. Illustration of different scenarios for the moraine breach at Ventisquero Negro. Depending on the outburst scenario the GLOF occurred as a result of progressive breach enlargement or through partial dam collapses with rapid breach enlargement.

Table 1
Model parameters, values as used for the dam break simulation with BASEMENT, parameter sensitivity and data sources (F = field measurement, M = material constant, C = calibration factor). Values in parenthesis indicate the range of parameter values for the sensitivity analysis.

Parameter	Description	Sensitivity	Values for modeling	Source
Rho Fluid	Fluid density	Low	1000 kg/m^3 (1100 kg/m^3)	M
Manning's roughness n	Resistance factor including bed and macroform roughness and internal energy dissipation	High	0.05 s/m$^{1/3}$ (0.07 s/m$^{1/3}$)	F/M
Sediment transport formula	Empirical equation to calculate sediment transport	Moderate	Modified MPM	
Grain Class	Diameters of all grains of the bed/dam material	Low	1, 8, 22, 64, 128, 180 mm (0.5, 4, 11, 32, 64, 90 mm)	F[b]
Mixture (moraine)	Fraction of each grain class	Low	11%, 17%, 24%, 24%, 14%, 10%	F[b]
Porosity	General bed material porosity	High	15% (25%)	M [a]
Density	General density of the bedload	Low	2650 kg/m^3 (2400 kg/m^3)	M
Bedload factor	Linear multiplication of transport capacity	High	1 (1.5)	C
Control volume thickness	Thickness of the uppermost layer where the bedload transport occurs	Moderate	0.05 m (0.1 m)	C
Failure angle below water surface	Angle at which a slope failure occurs when below water (similar to the angle of repose)	High	45° (40°)	F[c]
Failure angle above water surface	Angle at which a slope failure occurs when above water (often much larger than the angle of repose)	Moderate	82° (77°)	F[c]
Failure angle of deposition	Slope failure angle for deposited material after transport	High	15° (20°)	C

[a] Parriaux and Nicoud (1990).
[b] Based on Fig. 2.
[c] Explained in detail in Section 5.1.

whereas all other zones in the model domain were defined as non-erodible.

6.2. Model results

The model domain, initial conditions and input parameters (see Table 1) were used to model the breach of the Ventisquero Negro end moraine and subsequent lake drainage with BASEMENT. The modeled breach evolution shows that the steepest section of the moraine, some 150 m below the outlet, experienced most initial erosion, which caused the downstream face of the dam to steepen at this point (Fig. 7B; 30 min). The resulting rapid flow in the steep section entrained more bedload and the breach evolved backward towards the outlet. This knickpoint retreat resulted in a lowering of the lake outlet and in increased discharge, thus leading to progressive vertical and horizontal breach enlargement (Fig. 7B; 60 and 120 min). Model results also indicate that higher flow velocities occurred as a result of increasing outflow and that the maximum value of 17 m s^{-1} was reached at 70 min after the simulation was started. With increasing flow velocities bottom shear stress increased simultaneously to a maximum of 5100 N m^{-2}, which in turn enhanced erosion rates and vertical breach growth. Breach deepening resulted in steepening of the side walls, which collapsed as soon as critical failure angles were exceeded, leading to breach widening. The simulation of the growing breach cross-section allowed more outflow and progressive dam erosion. The model also suggests that deposition rates in the flood plain below the breach are directly correlated with breach expansion. The model run ended after 180 min when the lake level and outflow decreased below the threshold for bedload transport and breach expansion ceased.

The positive feedback loop as described above resulted in an exponential increase in discharge. During the first 45 min of the simulation discharge increased constantly up to 700 m^3 s^{-1}, before it steeply rose to a maximum of 4100 m^3 s^{-1} after 80 min. The outflow hydrograph showed a steep falling limb which became flatter after 120 min and eventually returned to nearly normal outflow. The model runs also indicate that the complete water volume of 10×10^6 m^3 was released within 180 min (Fig. 7A).

6.3. Model output validation

Model outputs were validated through comparison between modeled and measured breach and deposition geometry as well as lake level drop; it was assumed that a good match implies a reasonable reproduction of breach expansion rates.

Satellite imagery and field evidence clearly show a longitudinally curved breach whereas the modeled breach is straight but

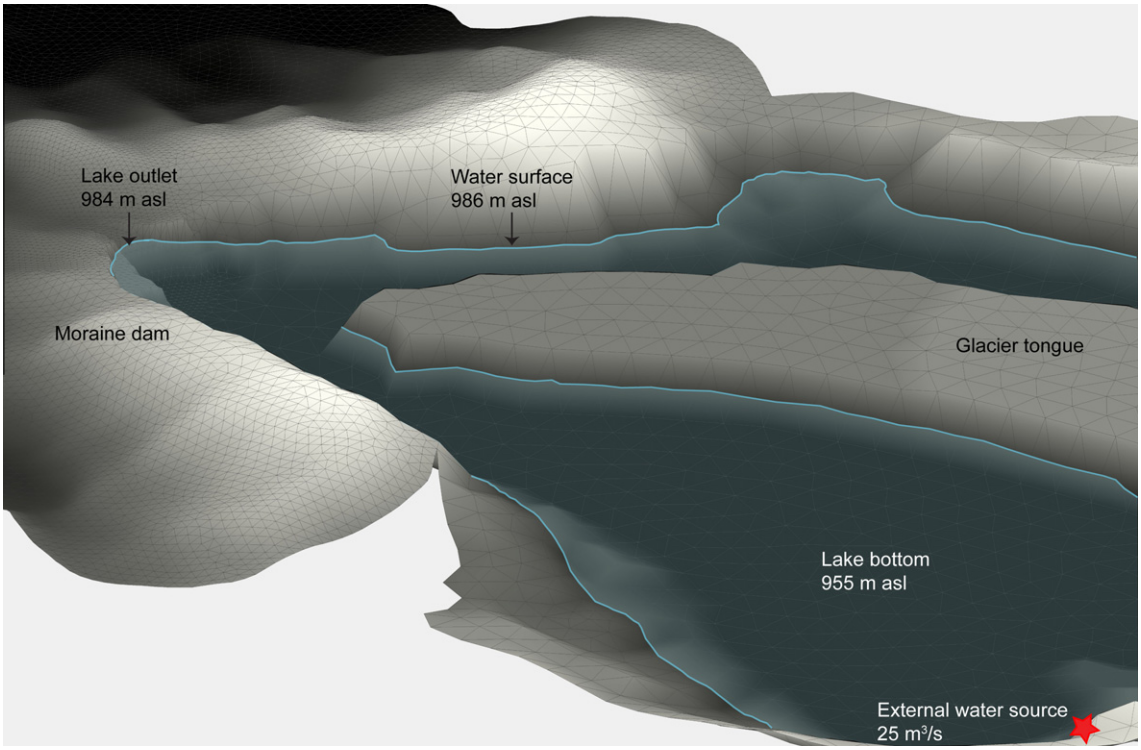

Fig. 6. The lake bathymetry, the topography of the moraine and the surrounding terrain is the model domain, represented by a mesh of triangular cells. The water surface elevation and external water source are the model's initial conditions.

of similar extent. At the upper and lower end of the breach (points 1 and 7 in Fig. 8), the actual breach was ca. 5–7 m deeper than modeled (see inset in Fig. 8); otherwise, measured and modeled breach depths coincide well, with a mean deviation of 2.5 m. The model calculated a drop in lake level of 30 m with 1 m water depth remaining in the basin; field measurements indicate a lake level drop by ca. 27 m and ca. 5 m water depth remaining in the basin. Fieldwork revealed that the eroded dam material was transported by debris flows and deposited in two different zones (see dotted yellow[3] lines in Fig. 8) with maximum thicknesses of 15 m some 120 m below the moraine. In BASEMENT all deposition of material occurs in the upper runout zone and the model suggests maximum deposition heights of 18 m ca. 280 m downstream of the moraine (Fig. 8). However, as the flow physics modeled in BASEMENT do not account for sediment motion as debris flow, differences in deposition between model and reality are not unexpected in this study.

Eyewitness reports indicate that the inundation at Pampa Linda lasted for 7 ± 2 h. The duration of the dam breach and lake outflow processes cannot, however, easily be compared with the time reported for the inundation because (i) flood attenuation effects might have increased the flood duration, and (ii) water presumably drained slowly on the large and flat valley plain at Pampa Linda. Hence, as there are no data on lake outflow duration and lake discharge the outflow hydrograph (as suggested by BASEMENT) can only be validated indirectly.

7. Discussion

The application of erosion-based, dynamic dam break models to real case events is still in the early stages of development. Advances in this field of study are essential, as a proper modeling technique for moraine breaching is crucial to assess the hazard potential of existing glacier lakes, which to date is often limited to qualitative studies. Studies on past GLOFs and on outburst prone lakes exist for many mountain regions in the world, but few glacier lakes and GLOF events have been systematically analyzed in the Patagonian Andes (e.g. Dussaillant et al., 2010). More particularly, studies on lake outbursts, caused by moraine failure, are rare for this region (Harrison et al., 2006). The Ventisquero Negro case study provides original information from a poorly studied area and sheds light on a natural hazard that might become increasingly relevant in Patagonia, especially with respect to possible hydropower projects (Vince, 2010).

GLOF disasters are characterized by complex and interacting processes, typically resulting from cascades of processes rather than single phenomena (Haeberli et al., 2010). This was observed at Ventisquero Negro, where, in addition to heavy rainfall, two long-term processes may have contributed to trigger the failure of the moraine: (i) accelerated lake growth observed in the years preceding the outburst resulted in a steadily increasing hydrostatic pressure on the dam; and (ii) a gradual reduction of stability of the end moraine occurred as the ice core abutting the moraine progressively melted following loss of glacier contact. Hence, the stability of the moraine-lake system at Ventisquero Negro progressively decreased and the high lake outflow in May 2009 eventually triggered dam incision.

Based on field evidence and model results, the following dam breaching process seems plausible: Dam incision due to heavy lake outflow started at the lake outlet (or even below), which was downstream of the ice core (Fig. 9A). The outflowing water eroded the steepest part of the moraine initially and progressively incised back towards the ice core. The curved plan of the breach geometry around the ice block and the absence of ice on the orographic right side of the breach (Fig. 9B) indicate that water followed the path of

[3] For interpretation of color in Fig. 8, the reader is referred to the web version of this article.

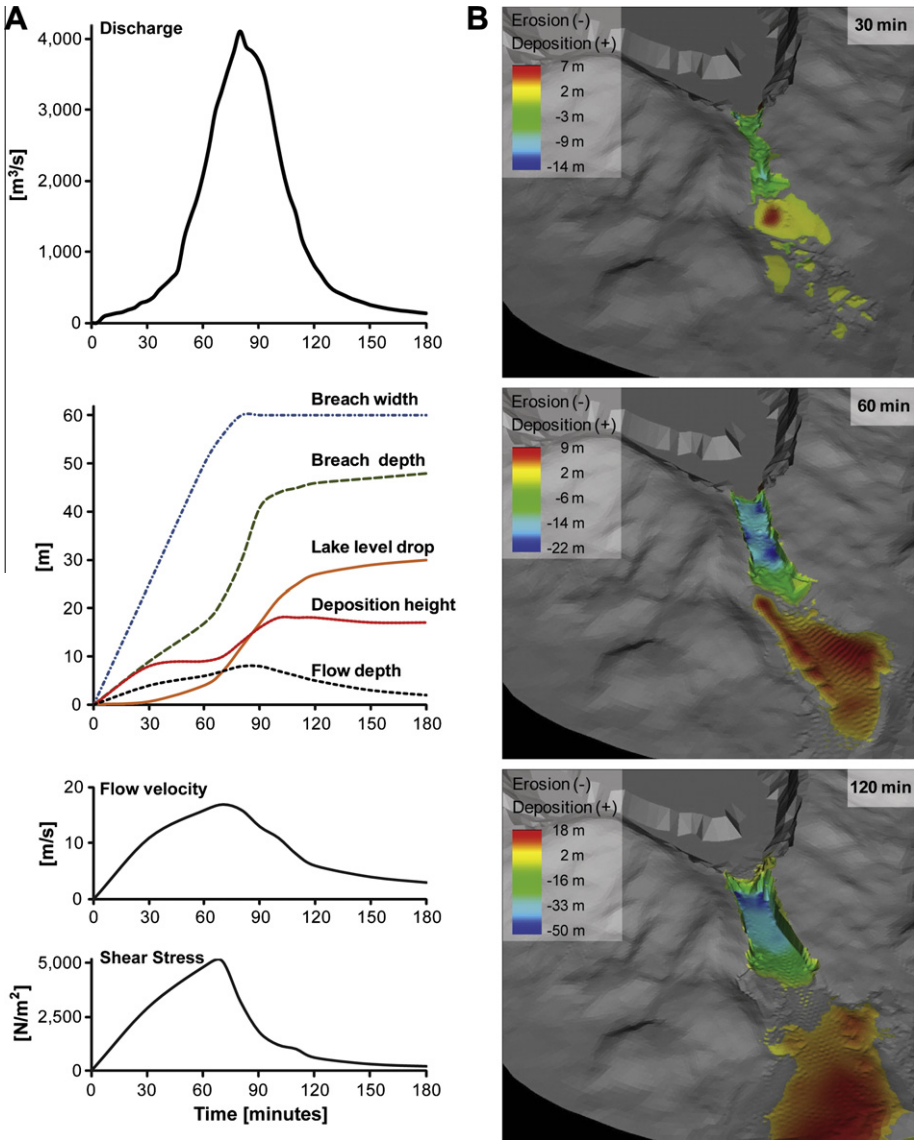

Fig. 7. Model results. (A) Temporal evolution of discharge, breach expansion, lake level drop, deposition, flow velocity and bottom shear stress as developed in the dam break model BASEMENT. All output parameters increase to maximum values 60–90 min after the run was started. (B) Visualization of breach expansion and deposition with three stationary shots at 30, 60, and 120 min.

minimal resistance to erosion (which is not the ice) and incised the sediment around the ice block, which then failed due to stress changes. Fragments of the ice core and floating ice blocks partly blocked the uppermost passage of the breach (Fig. 9B). Although this ice barrier was still water-permeable it reduced vertical and horizontal erosion rates. This resulted in forcing of the thalweg towards the ice-free part of the dam where incision and lateral bank collapse dominated. Similar developments of moraine breaches are described in the literature (Clague and Evans, 2000; Richardson and Reynolds, 2000b; Coleman et al., 2002; Hancox et al., 2005; Osti et al., 2011).

As there was evidence for a progressive breach formation driven by the water's sediment transport capacity, we decided to test the dynamic, erosion-based dam break model BASEMENT for the first time under case-study conditions. Model calibration and validation were challenging as a result of the limited data availability and was therefore done primarily via the geometry of the final breach; nevertheless model results were consistent with field observations. As a result of limited data, an uncertainty analysis of four critical model inputs was particularly important in view of the difficulties prevailing for modeling real-case dam breaches in general:

(i) The quality of model results strongly depends on the accuracy of reconstructed dam and lake geometry, which are based on the DEM and field mapping. DEM data for Ventisquero Negro were of unusually high resolution (7 m) for such a remote location, however, some irregularities and inaccuracies along the flow path and at the moraine still persisted in the DEM and directly affected model results (e.g. breach position, breach evolution, or lake discharge).

(ii) The model's initial conditions (lake water surface elevation and lake bathymetry; inflow hydrograph) have considerable uncertainties and are based partly on field observations (e.g. lake bathymetry), as well as on a trial-and error approach. The latter approach aimed at the identification of an initial water surface elevation of the lake high enough to result in a complete dam failure.

(iii) Since the ice body could not be considered in the dam break model, erosion rate and final cross-section geometry were slightly overestimated in the simulation for the upstream end of the breach. The smaller cross-sectional area observed in the field compared to model output also controlled max-

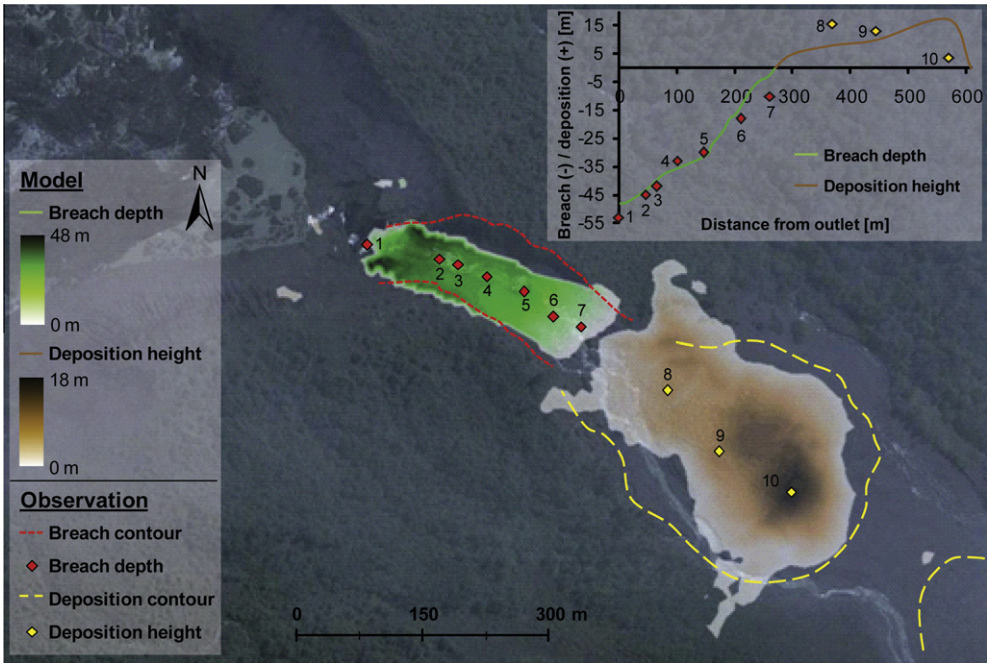

Fig. 8. Validation of model results based on a comparison between measured and modeled breach and deposition geometries. BASEMENT calculated breach depths and extent (green) are similar to those observed in the field. In contrast, modeled deposition of all material (brown) occurred in the first debris flow depositional zone. (For interpretation of the references to colour in this figure legend, the reader is referred to the web version of this article.)

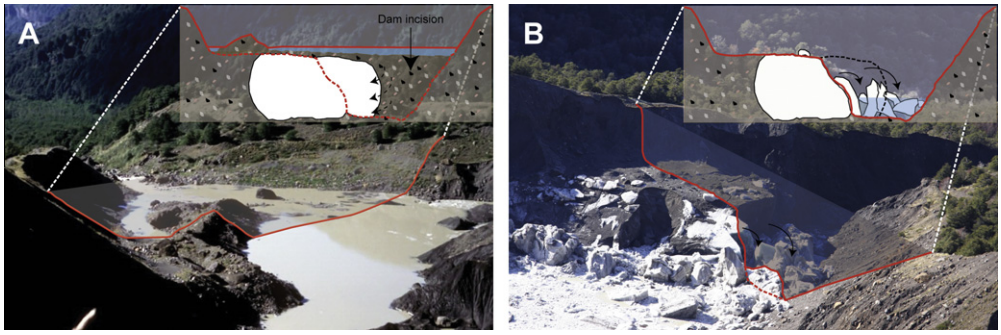

Fig. 9. The ice core abutting the Ventisquero Negro end moraine before (A) and after (B) the dam failure (same position of cross-sections). Note that the lake outlet was behind the ice body prior to lake drainage. The outflowing water incised predominantly on the right side of the ice and ruptured it laterally.

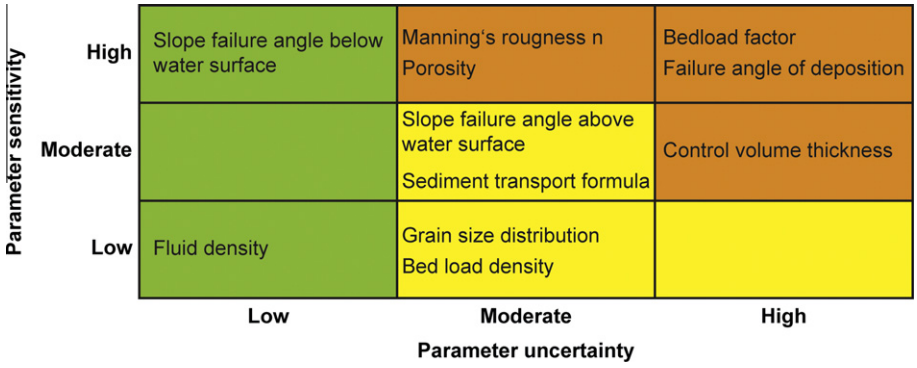

Fig. 10. BASEMENT input parameters, qualitatively categorized according to their sensitivity and uncertainty. Green parameters are marginally critical, yellow parameters are moderately critical and orange parameters are critical regarding the robustness of the model output. (For interpretation of the references to colour in this figure legend, the reader is referred to the web version of this article.)

imum water discharge from the lake. It seems likely therefore that BASEMENT slightly overestimated the largest outflow values.

(iv) In BASEMENT, physically-based input parameters controlled breach formation, and the calibration parameters (i.e. bedload factor, failure angle of deposition, control volume thick-

ness) allowed minor adjustments to achieve a good match with reality. The definition of calibration parameters is challenging and must be adjusted through retrospective modeling of a past event. At Ventisquero Negro no multiplication factor was required for bedload capacity, even though the MPM equation used was defined for rather flat terrains with uniform flow conditions (Smart, 1984). The deposition angle has been shown to correspond to about half the repose angle of the dam material in a simulation by laboratory experiment (Volz et al., 2010). Yet, for the modeling of the moraine breach at Ventisquero Negro, a value representing one-third of the repose angle appeared more appropriate. Also, the default value of 0.1 m for the control volume thickness resulted in exaggerated erosion rates and in an unrealistic breach shape; a value of 0.05 m resulted in a much better agreement between model output and reality.

Parameters such as Manning's n roughness value, porosity, grain size distribution and slope failure angles are based on field data and values proposed in literature (e.g. Parriaux and Nicoud, 1990; USGS, 2012) and are therefore less poorly constrained.

The influence of an input parameter on model robustness can be assessed by comparing parameter uncertainty with its sensitivity in the model: The higher parameter sensitivity and uncertainty, the more critical it will be for the quality of the model output. Fig. 10 presents the most important model input parameters, qualitatively categorized according to their sensitivity and uncertainty. This information helps to identify the most relevant parameters when calibrating dam break simulations with BASEMENT.

When considering the parameter uncertainties and limitations of the model, BASEMENT is appropriate and valuable for hazard assessments of existing glacier lakes, provided it was previously carefully calibrated. The modeling approach presented in this paper can be applied to quantify lake outburst scenarios and to assess GLOF impacts at other locations. The availability of critical dam breach parameters will facilitate the planning and dimensioning of accurate mitigation measures and help the justification of decisions aimed at preserving infrastructure and populated areas from possible GLOF risks.

8. Conclusions

The detailed reconstruction of the Ventisquero Negro moraine breach is one of a very few case studies on a topic that is gaining increasing attention due to ongoing glacier retreat and lake formation. In principle, different outburst scenarios are possible in the present case, but field evidence and model results suggest that high lake outflow initiated significant bedload transport and dam erosion, leading to progressive breach enlargement and lake outflow. The field-based reconstruction of the Ventisquero Negro moraine failure provided valuable input data for the simulation of the breaching event and allowed calibration and validation of the dynamic BASEMENT model. The simulation, based on sediment transport laws, provided detailed insights into dam breach processes that are difficult to observe in nature and results were largely consistent with field evidence. As the model seemed to reproduce the lake outflow hydrograph accurately, we suggest that dynamic models such as BASEMENT could be implemented systematically in the future to define outburst scenarios for unstable moraine-dammed lakes. More investigations on moraine failure processes and dam break model applications are needed to further improve the quality of model output and other trigger mechanisms, such as overtopping impact waves, should be included in dam break modeling. This can provide information on the conditions under which dam failures occur, both in the model environment and reality. It is known that melting ice cores in moraines make dams more susceptible to failure and therefore, with ongoing climate change GLOF potential may increase. Several situations similar to Ventisquero Negro exist and in order to accurately assess GLOF risks, further research should focus on dam break modeling where the effect of ice is considered.

Acknowledgements

We would like to thank Ricardo Villalba and Mariano Masiokas (IANIGLA) for their invitation to work in Patagonia. Special thanks are addressed to all other persons from IANIGLA who supported us in different ways within the present study. We appreciate the work from Diego Vallmitjana for the DEM generation. Ramón Chiocconi (Club Andino Bariloche) provided photographs taken from a helicopter shortly after the GLOF. This study was realized within the EU-FP7 project "HighNoon". We appreciate the constructive reviews of Vern Manville, two anonymous reviewers and Konstantine P. Georgakakos.

References

Ashida, K., Michiue, M., 1971. An investigation over river bed degradation downstream of a dam. In: Proceedings 14th Congress of IAHR, Paris, France, pp. 247–256.

Balmforth, N.J., Hardenberg, J.V., Provenzale, A., Zammett, R., 2008. Dam breaking by wave-induced erosional incision. J. Geophys. Res. 113, 1–12.

Carey, M., 2005. Living and dying with glaciers: people's historical vulnerability to avalanches and outburst floods in Peru. Global Planet. Change 47 (2–4), 122–134.

Carey, M., Huggel, C., Bury, J., Portocarrero, C., Haeberli, W., 2011. An integrated socio-environmental framework for glacier hazard management and climate change adaptation: lessons from Lake 513, Cordillera Blanca, Peru. Clim. Change. http://dx.doi.org/10.1007/s10584-011-0249-8.

Carrivick, J.L., Manville, V., Cronin, S.J., 2009. A fluid dynamics approach to modelling the 18th March 2007 lahar at Mt. Ruapehu, New Zealand. Bull. Volcanol. 71, 153–169.

Clague, J., Evans, S.G., 1994. Formation and failure of natural dams in the Canadian Cordillera. Geol. Soc. Can. Bull. 464, 35 pp.

Clague, J.J., Evans, S.G., 2000. A review of catastrophic drainage of moraine-dammed lakes in British Columbia. Quat. Sci. Rev. 19, 1763–1783.

Clarke, G.K.C., 1982. Glacier outburst floods from 'Hazard Lake', Yukon Territory, and the problem of flood magnitude prediction. J. Glaciol. 28 (98), 3–21.

Coleman, S.E., Andrews, D.P., Webby, M.G., 2002. Overtopping breaching of noncohesive homogeneous embankments. J. Hydrol. Eng. 128 (9), 829–838.

Costa, J.E., Schuster, R.L., 1988. The formation and failure of natural dams. Geol. Soc. Am. Bull. 100, 1054–1068.

Dussaillant, A., Benito, G., Buytaert, W., Carling, P., Meier, C., Espinoza, F., 2010. Repeated glacial-lake outburst floods in Patagonia: an increasing hazard? Nat. Hazards 54 (2), 469–481.

Evans, S.G., 1986. The maximum discharge of outburst floods caused by the breaching of man-made and natural dams. Can. Geotech. J. 23, 385–387.

Faeh, R., 2007. Numerical modeling of breach erosion of river embankments. J. Hydrol. Eng. 133 (9), 1000–1007.

Faeh, R., Mueller, R., Rousselot, P., Veprek, R., Vetsch, D., Volz, C., Vonwiller, L., Farshi, D., 2011. BASEMENT – Basic Simulation Environment for Computation of Environmental Flow and Natural Hazard Simulation. VAW, ETH Zurich. <http://www.basement.ethz.ch>.

Fread, D.L., 1991. BREACH: An Erosion Model for Earthen Dam Failures. Hydrologic Research Laboratory, National Weather Service, National Oceanic and Atmospheric Administration, Silver Spring, MD.

Frey, H., Haeberli, W., Linsbauer, A., Huggel, C., Paul, F., 2010. A multi-level strategy for anticipating future glacier lake formation and associated hazard potentials. Nat. Hazards Earth Syst. Sci. 10, 339–352.

Haeberli, W., Clague, J.J., Huggel, C., Kääb, A., 2010. Hazards from lakes in high-mountain glacier and permafrost regions: climate change effects and process interactions. Avances de la Geomorphología en España, 2008–2010, XI Reunión Nacional de Geomorphología, Solsona, pp. 439–446.

Hahn, W., Hanson, G.J., Cook, K.R., 2000. Breach morphology observations of embankment overtopping tests. In: Proceedings of the 2000 Joint Conference on Water Resources Engineering and Water Resources Planning and Management, ASCE, July 30–August 2, MN, USA.

Hancox, G.T., McSaveney, M.J., Manville, V., Davies, T.R., 2005. The October 1999 Mt Adams rock avalanche and subsequent landslide dam-break flood and effects in Poerua River, Westland, New Zealand. N.Z. J. Geol. Geophys. 48, 683–705.

Harrison, S., Glasser, N., Winchester, V., Haresign, E., Warren, C., Jansson, K., 2006. A glacial lake outburst flood associated with recent mountain glacier retreat, Patagonian Andes. Holocene 16 (4), 611–620.

Hewitt, K., 1982. Natural dams and outburst floods of the Karakoram Himalaya. In: Glen, J.W. (Eds.), Hydrological Aspects of Alpine and High Mountain Areas. Association of Hydrological Sciences (IAHS), pp. 259–269.

Huggel, C., Haeberli, W., Kääb, A., Bieri, D., Richardson, S., 2004. An assessment procedure for glacial hazards in the Swiss Alps. Can. Geotech. 41, 1068–1083.

IPCC, 2007. Climate change 2007 synthesis report. In: Pachauri, R.K., Reisinger, A. (Eds.), Contribution of Working Groups I, II and III to the Fourth Assessment Report of the Intergovernmental Panel on Climate Change. IPCC, Geneva, 104 pp.

Jorgenson, J., Xinya, Y., Woodman, W., 2004. Two-dimensional Modeling of Dam Breach Flooding. US–China Workshop On Advanced Computational Modelling in Hydroscience & Engineering, 19–21 September, Oxford, Mississippi, USA, 2004.

Kershaw, J.A., Clague, J.J., Evans, S.G., 2005. Geomorphic and sedimentological signature of a two-phase outburst flood from moraine-dammed Queen Bess Lake, British Columbia, Canada. Earth Surf. Process. Landforms 30, 1–25.

Korup, O., Tweed, F., 2007. Ice, moraine, and landslide dams in mountainous terrain. Quat. Sci. Rev. 26, 3406–3422.

Malone, E., 2010. Changing Glaciers and Hydrology in Asia: Addressing Vulnerabilities to Glacier Melt Impacts. USAID, Washington, November 2010. <http://www.usaid.gov/locations/asia/documents/Asia_Glacier_Melt_Vulnerability_Nov-2010.pdf> (accessed 03.01.12).

Masiokas, M.H., Luckman, B.H., Villalba, R., Ripalta, A., Rabassa, J., 2010. Little Ice Age fluctuations of Glacier Río Manso in the north Patagonian Andes of Argentina. Quat. Res. 73, 96–106.

Massey, C., Manville, V., Hancox, G.T., Keys, H.J.R., Lawrence, C., McSaveney, M.J., 2010. Out-burst flood (lahar) triggered by retrogressive landsliding, 18 March 2007 at Mt. Ruapehu, New Zealand – a successful early warning. Landslides 7, 303–315.

Meon, G., Schwarz, W., 1993. Estimation of glacier lake outburst flood and its impact on a hydro project in Nepal. In: Young, G.J. (Ed.), Snow and Glacier Hydrology. IAHS, Oxford, pp. 331–339.

Mergili, M., Schneider, D., Worni, R., Schneider, J.F., 2011. Glacial Lake outburst Floods (GLOFs): challenges in prediction and modelling. In: Proceedings of the 5th International Conference on Debris-Flow Hazard Mitigation: Mechanics, Prediction and Assessment, Padua, Italy, 14–17 June, 2011. doi: http://dx.doi.org/10.4408/IJEGE.2011-03.B-106.

Meyer-Peter, E., Müller, R., 1948. Formulas for bed-load transport. Int. Assoc. Hydrol., Res., 2nd Congr. Proc., Stockholm, pp. 39–64.

Osti, R., Egashira, S., 2009. Hydrodynamic characteristics of the Tam Pokhari Glacial Lake outburst flood in the Mt. Everest region, Nepal. Hydrol. Process. 23, 2943–2955.

Osti, R., Bhattarai, T.N., Miyake, K., 2011. Causes of catastrophic failure of Tam Pokhari moraine dam in the Mt. Everest region. Nat. Hazards 58, 1209–1223.

Parriaux, A., Nicoud, G.F., 1990. Hydrological behaviour of glacial deposits in mountainous areas. Hydrol. Mountain Areas IAHS 190, 291–311.

Pickert, G., Weitbrecht, V., Bieberstein, A., 2011. Breaching of overtopped river embankments controlled by apparent cohesion. J. Hydraul. Res. 49 (2), 143–156.

Richardson, S.D., Reynolds, J.M., 2000a. An overview of glacial hazards in the Himalayas. Quat. Int. 65 (66), 31–47.

Richardson, S.D., Reynolds, J.M., 2000b. Degradation of ice-cored moraine dams: implications for hazard development. In: Nakawo, M., Raymond, C.F., Fountain, A. (Eds.), Debris-covered Glaciers, IAHS Red Book Series, pp. 187–198.

Shields, A., 1936. Anwendung der Aehnlichkeitsmechanik und der Turbulenzforschung auf die Geschiebebewegung. Mitt. Nr. 87, Versuchsanstalt für Wasser- und Schiffbau, Berlin.

Singh, V.P., 1996. Dam Breach Modelling Technology, vol. 17. Kluwer Academic Publishers., Dordrecht, Boston, London, 242 pp.

Singh, V.P., Scarlatos, P.D., 1985. Breach Erosion of Earthfill Dams and Flood Routing: BEED Model. Research Report, Army Research Office, Battelle, Research Triangle Park, North Carolina, 131 pp.

Smart, G.M., 1984. Sediment transport formula for steep channels. J. Hydraul. Eng. 110 (3), 267–276.

SMS, 2012. <http://www.scisoftware.com/products/sms_details/sms_details.html> (accessed 03.01.12).

Stoffel, M., Huggel, C., 2012. Effects of climate change on mass movements in mountain environments. Prog. Phys. Geog., in press. http://dx.doi.org/10.1177/0309133312441010.

Tingsanchali, T., Chinnarasri, C., 2001. Numerical modelling of dam failure due to flow overtopping. Hydrol. Sci. J. 46 (1), 113–130.

Toro, E.F., 2001. Shock-capturing Methods for Free-surface Shallow Flows. John Wiley and Sons, New York, 314 pp.

USGS, 2012. Verified Roughness Characteristics of Natural Channels. <http://wwwrcamnl.wr.usgs.gov/sws/fieldmethods/Indirects/nvalues/index.htm> (accessed 03.01.12).

Valiani, A., Caleffi, V., Zanni, A., 2002. Case study: Malpasset Dam break Simulation using a two-dimensional finite volume method. J. Hydraul. Eng. 128 (5), 460–472.

Villalba, R., Boninsegna, J.A., Veblen, T.T., Schmelter, A., Rubulis, S., 1997. Recent trends in tree-ring records from high elevation sites in the Andes of northern Patagonia. Clim. Change 36, 425–454.

Vince, G., 2010. Dams for Patagonia. Science 329 (5990), 382–385.

Volz, C., Rousselot, P., Vetsch, D., Mueller, R., Faeh, R., Boes, R., 2010. Numerical modeling of dam breaching processes due to overtopping flow. In: Proc. 8th ICOLD European Club Symposium 2010, Innsbruck, pp. 691–696.

Walder, J.S., Costa, J.E., 1996. Outburst floods from glacier-dammed lakes: the effect of mode of lake drainage on flood magnitude. Earth Surf. Process. Landforms 21, 701–723.

Watanabe, T., Rothacher, D., 1996. The 1994 Lugge Tsho Glacial lake outburst flood, Bhutan Himalaya. Mt. Res. Dev. 16 (1), 77–81.

Worni, R., Huggel, C., Stoffel, M., Pulgarín, B., 2011. Challenges of modeling current very large lahars at Nevado del Huila Volcano, Colombia. Bull. Volcanol. http://dx.doi.org/10.1007/s00445-011-0522-8.

Xin, W., Shiyin, L., Wanqin, G., Junli, X., 2008. Assessment and simulation of glacier lake outburst floods for Longbasaba and Pida Lakes, China. Mt. Res. Dev. 28 (3/4), 310–317.